

Radiative muon capture in a relativistic mean field theory: Fermi gas model

Harold W. Fearing

TRIUMF, Vancouver, British Columbia, Canada V6T 2A3

G. E. Walker

Nuclear Theory Center and Department of Physics, Indiana University, Bloomington, Indiana 47405

(Received 28 September 1988)

We examine radiative muon capture in a nuclear medium using mean field theory and a relativistic Fermi gas model for the nucleus to obtain the single nucleon states. The aim is to explore, in a simple model, effects of the medium which are characterized primarily by a nucleon effective mass m^* , as well as other relativistic effects. The relative rate, i.e., the photon spectrum divided by the nonradiative rate, and the photon asymmetry relative to the muon spin are calculated. The most important effect turns out to be the Fermi motion which reduces the relative rate by a factor of 2–3 in the experimentally accessible region, compared to the static case. The m^* effect further reduces the result by 10–50%, depending on the photon energy. The relativistic nature of this calculation, unlike usual nonrelativistic calculations, allows these effects to be incorporated to all orders in $1/m$. As a consequence some interesting effects can be studied in the small k region. We conclude that both relativistic kinematic and medium effects may be significant and thus that it is worthwhile investigating this reaction in more realistic relativistic nuclear models.

I. INTRODUCTION

There has been a lot of interest recently in relativistic mean field theory approaches to problems involving a variety of medium energy processes in nuclei.¹ Recall that in such theories the effects of the nuclear medium are incorporated via very strong effective average scalar and vector potentials. The nucleon field satisfies a Dirac equation in the presence of these potentials. One important qualitative effect of such potentials is a renormalization of the nucleon mass in the medium which is brought about by the scalar potential. Thus in the medium the free nucleon mass $m \rightarrow m^*$ where the effective mass m^* can be of the order of $0.6m$.

One is then immediately led to the question of whether one can see effects of this mass renormalization in nuclear processes. A related question is whether one can see effects which can be traced to the relativistic nature of the approach. This question has been asked with respect to a variety of proton scattering reactions,² to ordinary, nonradiative, muon capture, to beta decay, and to electron scattering,³ with somewhat mixed results. Sometimes there are moderately large effects and sometimes only fairly small ones. The purpose of the present paper is to ask this same question with respect to radiative muon capture.

The backflow effects associated with higher-order corrections to the relativistic wave function have been shown to be important for isoscalar transitions.^{4–6} Such corrections are suppressed for isovector transitions⁶ such as those associated with muon capture and thus such processes are attractive to study.

Why else might radiative muon capture be interesting as a laboratory for investigating relativistic and effective mass effects? In the first place one might expect radiative

muon capture to be more sensitive than some processes to relativistic effects in the model. This possibility is suggested by the fact that radiative muon capture, like ordinary muon capture but unlike beta decay, depends on the induced weak interaction coupling constants. In particular, radiative capture is very sensitive to the induced pseudoscalar coupling g_p which is given by the Goldberger-Treiman relation. Sensitivity to the induced couplings is important since these are terms of order $1/m$, and thus in some sense relativistic corrections.

The effects of the medium may also be important in radiative muon capture. Such effects, originating in the effective mass m^* , enter in two places. First, since $m^* < m$, they will enhance all of the relativistic type terms, which are of the form p/m . Second, m^* will appear in the numerator of the g_p terms since the Goldberger-Treiman relation, applied in the medium, indicates that g_p is proportional to $2m^*g_A$.³ Thus, at least for these terms, some of the m^* effects may cancel. However, since there are many such terms with different signs, it is necessary to actually do a calculation to really determine the effect of either relativistic or m^* terms.

The purpose of this article is thus to carry out such a calculation in a very simple model, namely, a relativistic Fermi gas. While such a model is obviously oversimplified and cannot be expected to give quantitative information relevant to real nuclei, it should give some idea of the size of the various effects and some indication of the value of a calculation involving more detailed models.

In the next section we review the standard approach to radiative muon capture for a free proton.⁷ The following section describes the features of the relativistic mean field theory which will be required. Next we describe how these two ingredients are combined to obtain a calcula-

tion of both the photon spectrum and the asymmetry relative to the muon spin. The final sections describe our results and some of the interesting features which emerge.

II. RADIATIVE MUON CAPTURE ON A FREE PROTON

In this section we review the standard theory of radiative muon capture as applied to the free proton. We are thus considering the process $\mu + p \rightarrow n + \nu + \gamma$. Notation will be that of Ref. 7, and, in particular, we shall use the particle symbols to stand for their four-momenta and use m_p, m_n, m_μ for the respective free masses.

The usual contributions to this process are depicted in Fig. 1 and correspond to radiation from the muon, from the proton via both charge and magnetic moment and from the neutron via its magnetic moment. Figure 1(d) corresponds to radiation from the virtual pion which generates the induced pseudoscalar coupling and Fig. 1(e) is a gauge term arising because of the momentum dependence of the weak vertex. The weak vertices contain vector and axial vector couplings, g_V and g_A , and as well the weak magnetism term g_M and induced pseudoscalar term g_P .

For the calculation considered here we will need the matrix elements corresponding to these diagrams evaluated for free Dirac spinors. Such matrix elements are easily calculated using standard Feynman rules and are given explicitly in Eq. (1) of Ref. 7. The induced pseudoscalar coupling is defined as a function of momentum transfer as

$$g_P(q^2) = g_P(-m_\mu^2)(m_\pi^2 + m_\mu^2)/(m_\pi^2 - q^2)$$

with

$$g_P(-m_\mu^2) = m_\mu(m_p + m_n)g_A/(m_\pi^2 + m_\mu^2) \cong 6.6g_A$$

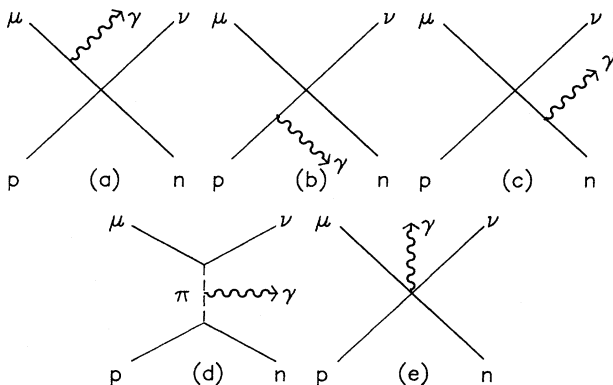


FIG. 1. Diagrams contributing to radiative muon capture on a proton: (a) radiation from the muon; (b) radiation from the charge and magnetic moment of the proton; (c) radiation from the magnetic moment of the neutron; (d) radiation from the exchanged pion which generates the induced pseudoscalar coupling; and (e) gauge term arising from the momentum dependence of the weak vertices.

being the Goldberger-Treiman value. For radiative muon capture q takes two different values depending on the diagram being considered. In particular one has $q = q_L = n - p$ for Figs. 1(a) and 1(e) and $q = q_N = n - p + k$ for Figs. 1(b) and 1(c). Figure 1(d) contains both. Of these, $q_L^2 \cong -m_\mu^2$, but q_N^2 can nearly reach $+m_\mu^2$, which leads to an enhancement of $g_P(q^2)$ of almost a factor of 4 and contributes to the sensitivity of radiative muon capture to the induced pseudoscalar coupling constant.

These are the important contributions to this matrix element, but there are some others which could be included. In particular some contributions of the $\Delta(1232)$ have been considered in Ref. 8. These seem to be small, however, and will be neglected here.

To evaluate the capture rate, one squares the matrix element and sums on spins in the standard fashion, and combines the result with the appropriate phase space factor. The muon is taken at rest and the appropriate hydrogenic muon wave function, evaluated at the origin, is multiplied into the matrix element. For the free proton, the calculation is usually done in the rest frame of the proton, so the proton is taken at rest as well. The actual quantities that can currently be measured are the photon spectrum $d\Gamma/dk$ and the asymmetry parameter $A(k)$ in the angular correlation

$$d^2\Gamma/dk d\cos\theta \sim 1 + A(k)\cos\theta,$$

where $\cos\theta$ is the angle between the muon spin and the photon direction. This, by now, rather standard procedure is described in detail in Ref. 7.

For the purposes of the present calculation this description of the process for relativistic free protons is sufficient as we plan to treat the nucleus as a relativistic Fermi gas. Thus in our case the extension to a nucleus will be a simple extension of the free single-particle calculation to the situation where the proton is not at rest, together with a sum over the set of single-particle states. To make contact with the existing more realistic, and invariably nonrelativistic, nuclear calculations, however, it is useful to review briefly the usual nonrelativistic approach for the nuclear case. In that case the free proton matrix element derived from the diagrams of Fig. 1 is first reduced to two-component form. The muon is taken at rest, but not the proton, and again the muon wave function at the origin is included. Then a nonrelativistic approximation is made, which normally consists of keeping terms only through $O(1/m)$, though terms of $O(1/m^2)$ were considered by Sloboda and Fearing.⁹ The result is an operator in two-component spin space containing terms like 1 , $\sigma \cdot \mathbf{v}$, and \mathbf{p}/m . Matrix elements are then taken using some appropriate nonrelativistic nuclear wave functions. Fermi motion is thus included to first order in \mathbf{p} via explicit matrix elements of the operator p . To obtain the photon spectrum or asymmetry parameter the matrix element is squared and phase space included in the usual way.

It is the usual practice to divide the radiative rate Γ by the ordinary nonradiative rate Λ_{ord} , calculated in the same model, as this is supposed to remove some of the dependence on the detailed nuclear model and give a

cleaner interpretation in terms of the weak couplings. While this is only partially effective in removing the model dependence (see, e.g., Ref. 10), we will use this standard procedure.

One of the earlier summaries of this approach for nuclei was given by Luyten, Rood, and Tolhoek¹¹ who used closure and simple harmonic oscillator nuclear wave functions. Other calculations¹² were done in a giant dipole resonance model of Foldy and Walecka¹³ and in a variety of other nuclear models some of which are described in a recent review.¹⁴

On the experimental side there have been a number of measurements of both photon spectrum and asymmetry parameter in nuclei.¹⁵ There is also an experiment in progress to measure the process for the first time on a free proton.¹⁶

We have now summarized briefly the standard approach to radiative muon capture. In the next section we will review those aspects of relativistic mean field theory which are required for the calculation we wish to make.

III. RELATIVISTIC MEAN FIELD THEORY

There has been a lot of attention directed recently toward the relativistic mean field theories of the nuclear medium¹ and a lot of effort devoted to exploring various aspects of such theories. In the simplest picture, which is all we will use here, the nuclear medium is described by very strong scalar and vector mean fields. A nucleon in the medium then is governed by the Dirac equation in the presence of these fields, in particular by a solution of the equation

$$[i\bar{\partial} - g_v\gamma^0 V_0 - m + g_s\phi_0]\psi = 0. \quad (1)$$

Here ϕ_0 and V_0 are the scalar and time component of the vector mean fields, which for the infinite nuclear matter case can be taken as constants. The couplings are g_s and g_v and together with the fields lead to potentials of about 330 MeV and 400 MeV, respectively.¹ If we assume a solution of the form

$$\psi = u(p, \lambda) e^{-iE^*t + i\mathbf{p}\cdot\mathbf{x} - ig_v V_0 t} \quad (2)$$

and substitute into Eq. (1) we obtain

$$[\gamma_0\boldsymbol{\gamma}\cdot\mathbf{p} + \gamma_0(m - g_s\phi_0)]u(p, \lambda) = E^*u(p, \lambda). \quad (3)$$

If we take $m^* = m - g_s\phi_0$ and $E^* = (\mathbf{p}^2 + m^{*2})^{1/2}$ then this equation looks just like the free Dirac equation and the solutions for $u(p, \lambda)$ are the usual free spinor solutions of momentum p and spin λ , only with the mass m replaced by m^* . Thus, in this approach individual nucleons are described as though they were free, but with an effective mass m^* .

IV. RMC IN INFINITE NUCLEAR MATTER

In this section we describe the model adopted herein to investigate m^* effects. We begin by assuming an infinite

nuclear medium. Thus the mean fields ϕ_0 and V_0 can be taken as constants. In the more realistic finite nucleus case these fields will be position dependent, and as a consequence the calculation would be much more complicated.³ The potential¹ $g_s\phi_0 \approx 400$ MeV so that the effective mass $m^* \approx 0.57m$. The nucleus is then a relativistic Fermi gas, with single-particle states represented by Eq. (2) with the usual spinor $u(p, \lambda)$, except with mass m^* , and with all proton (and neutron) states filled for $p \leq k_F$, where k_F is the Fermi momentum of approximately 280 MeV. Likewise the final neutron goes into a single-particle relativistic spinor state with $n \geq k_F$.

The basic single-particle matrix element is obtained by evaluating the relativistic expression, Eq. (1) of Ref. 7, using the wave functions in the medium. Thus the expression for M_{fi} is the same as before except now m is replaced by m^* in the spinors, in the nucleon propagators, and in the expression for the Goldberger-Treiman relation for g_p .³ The m which appears in the $1/2m$ normalizing factors in the weak magnetism term g_M and in the anomalous magnetic moment terms proportional to κ_p or κ_n is kept as m rather than m^* as these factors just define the units of the couplings. It is easy to show explicitly, within the context of this model, that this interaction taken between states in the medium leads to an exactly gauge invariant result.

This procedure as applied to the propagator deserves some further comment. The momentum space Feynman propagator associated with the Dirac equation in the medium, Eq. (1), is

$$S_F(q) = \frac{1}{\not{q} - g_v\gamma^0 V_0 - m^*}, \quad (4)$$

and it would appear that the simple prescription outlined in the previous paragraph would miss the $g_v\gamma^0 V_0$ term in the denominator. However, by writing out the matrix elements explicitly one can easily see that the extra time-dependent factor $e^{-ig_v V_0 t}$ in the solution, Eq. (2), just produces a shift in the energy, thus changing q_0 by exactly the amount needed to cancel this term. Thus, ignoring this term in the propagator and the factor $e^{-ig_v V_0 t}$ in the wave functions and just substituting $m \rightarrow m^*$ everywhere gives the correct and consistent answer.

The square of this single-particle matrix element, $\sum |M_{fi}|^2$ can be evaluated using the usual trace techniques. Even for the present problem, the situation is sufficiently complicated that this expression was evaluated numerically. Thus the matrix element M_{fi} was obtained by adopting a specific representation of the matrices and multiplying them numerically, just as was done in Ref. 7. The resulting number was then squared so as to obtain $\sum |M_{fi}|^2$.

The capture rate is then obtained by multiplying $\sum |M_{fi}|^2$ by the appropriate phase space and other standard factors and integrating over the final neutron and initial proton states. The result is

$$\Gamma = \frac{G_F^2 \alpha}{4\pi^2} \frac{3m_p m_n}{4\pi k_F^3} |\phi_\mu(0)|^2 \int_{k_{\min}}^{k_{\max}} dk \int_{(\cos\theta_k)_{\min}}^{(\cos\theta_k)_{\max}} d\cos\theta_k \int_{p_{\min}}^{k_F} dp \int_{k_F}^{n_{\max}} dn \int_0^{2\pi} d\phi_n \frac{E_n n p^2 k}{E_p E_n |\mathbf{n} + \mathbf{v}|} \frac{1}{4} \sum_{\text{spins}} |M_{fi}|^2. \quad (5)$$

In this equation $G_F = 1.137 \times 10^{-11} \text{ MeV}^{-2}$ is the Fermi constant, $\alpha = \frac{1}{137}$ is the fine-structure constant, and $|\phi_\mu(0)|^2$ is the muon wave function at the origin. For the few absolute rates quoted we have calculated $|\phi_\mu(0)|^2$ using the simple Bohr wave function for ^{40}Ca evaluated at the origin and then multiplied by a factor 0.44, as given by Sens,¹⁷ to account for the average over the nuclear volume. This wave function of course cancels in the ratio of radiative to ordinary non-radiative rates. It should be emphasized that this procedure defines a convenient normalization but does not necessarily make this a realistic calculation for ^{40}Ca . The various integration limits are complicated functions of the kinematics and are evaluated numerically. These limits are determined by the usual energy and momentum relations for a three-body final state together with the constraints $p \leq k_F$ and $n \geq k_F$.

We will for the most part divide out the ordinary nonradiative rate to suppress some of the sensitivity to the nuclear model. Thus we also need the ordinary rate which is given by

$$\Lambda_{\text{ord}} = G_F^2 \frac{3m_p m_n}{4\pi k_F^3} |\phi_\mu(0)|^2 \int_{p_{\text{min}}}^{k_F} dp \int_{k_F}^{n_{\text{max}}} dn \frac{E_\nu n p^2}{E_p E_n |\mathbf{n} + \mathbf{v}|} \frac{1}{4} \sum_{\text{spins}} |M_{fi}|^2. \quad (6)$$

Here $|M_{fi}|^2$ is that appropriate for ordinary capture. It is obtained from Ref. 7 with the same changes $m \rightarrow m^*$ as used for the radiative case.

For such a complicated integral as in Eq. (5) above it is important to have some numerical checks on the correctness of the calculation. We made the usual checks on the stability of the integral by varying the number of integration points. We also checked that in the limit $m^* \rightarrow m$ and $k_F \rightarrow 0$ the numerical result did in fact reduce to that for a free proton at rest as obtained in Ref. 7, as it should.

V. RESULTS AND DISCUSSION

In this section we examine the effects on the relative rate $R = (d\Gamma/dk)/\Lambda_{\text{ord}}$ produced by replacing m by m^* and by incorporating Fermi motion as reflected by a nonzero k_F . The weak couplings are taken as in Ref. 7 and in particular g_p is evaluated using the Goldberger-Treiman functional form given above.

Figure 2 shows, for both the relative rate and the asymmetry, the effect of replacing m by $m^* = 0.57m$ with $k_F = 0$. Taking $k_F = 0$ puts the initial proton at rest and thus removes effects of Fermi motion and isolates the m^* effect. One can see from the figure that the effect for both

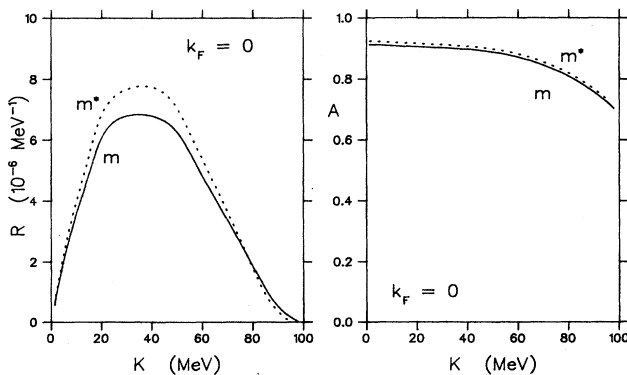


FIG. 2. Relative rate $R = (d\Gamma/dk)/\Lambda_{\text{ord}}$ and asymmetry parameter $A(k)$ for the limiting case $k_F = 0$, corresponding to the initial nucleon at rest, shown as a function of m^* . The solid curve uses the free m while the dotted curve corresponds to $m^* = 0.57m$. For orientation purposes, the ordinary rates calculated with the assumptions described in the text are, respectively, $\Lambda_{\text{ord}} = 8.93 \times 10^5 \text{ s}^{-1}$ and $\Lambda_{\text{ord}} = 8.23 \times 10^5 \text{ s}^{-1}$.

rate and asymmetry is not large. The rate does increase over most of the spectrum, by as much as 10% at the peak, as m decreases, but most of this comes from changes in Λ_{ord} .

Figure 3 shows the same curves over the range $k \geq 60$ MeV which is experimentally accessible. Shown also are the results for $k_F = 280$ MeV corresponding to nuclear matter. Clearly the Fermi motion effect is much larger than that due to m^* . The ordinary rate drops by a factor of more than 5 and the spectrum $d\Gamma/dk$ drops by an even larger factor. Also now the $m^* = 0.57m$ case is lower than the free nucleon mass case by as much as 30–50% above 70 MeV. Fermi motion reduces the asymmetry parameter as well, by about 10%. The reduction of the relative rate and the asymmetry parameter with increasing k_F is a fairly uniform one, as can be seen from Fig. 4 which shows these quantities for a series of values of k_F . Note that the Fermi motion effect is not an inherently relativistic concept. Such effects are present in most nonrelativistic calculations which keep terms through the first power in p . The advantage of the relativistic approach here is that all powers of the momentum are kept.

It is interesting to consider separately the two different

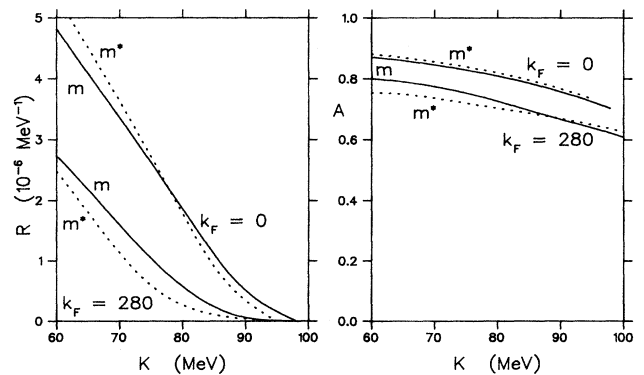


FIG. 3. Effect of Fermi motion and of $m \rightarrow m^*$ on the relative rate R and asymmetry parameter A in the experimentally accessible region $k \geq 60$ MeV. The upper curves are the $k_F = 0$ curves of Fig. 2. The lower curves have $k_F = 280$ MeV. For the latter the m and $m^* = 0.57m$ cases lead to Λ_{ord} values of $1.64 \times 10^5 \text{ s}^{-1}$ and $1.26 \times 10^5 \text{ s}^{-1}$, respectively.

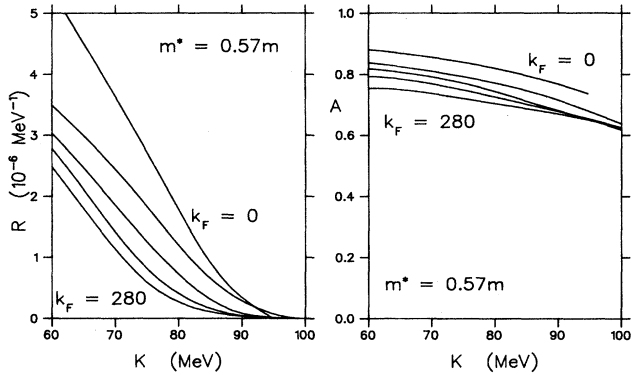


FIG. 4. Relative rate and asymmetry parameter in the experimentally accessible region as a function of k_F for $m^* = 0.57m$. Shown are results for $k_F = 0, 70, 140, 210,$ and 280 MeV.

sources of m^* effects which were described earlier. Introducing m^* everywhere except in g_p , i.e., in all of the $1/m$ type terms, leads for $k_F = 280$ MeV to a small suppression of the rate above 70 MeV and an enhancement below 70 MeV. Putting m^* in the numerator of g_p suppresses the rate everywhere. Thus the two effects together give the suppression seen in Fig. 3. For the asymmetry one can show¹⁸ that $1 - A \approx (g_p/m)^2 + \dots$ so that the two effects nearly cancel.

Another interesting feature of the relativistic calculation can be seen in Fig. 5 which shows the effect of the Fermi motion across the full photon spectrum. When the proton is at rest ($k_F = 0$) we see the usual spectrum shape which goes to zero at $k = 0$. Then as Fermi motion is turned on the spectrum develops a divergence at $k = 0$. This is of course not unexpected, since we know that in general a radiative process exhibits an infrared divergence. It has, however, not been evident in nonrelativistic calculations. The effect of this divergence on $A(k)$ is even more dramatic. $A(k)$ drops from nearly 1 to nearly 0 for small k as k_F goes from 0 to 280 MeV.

One can understand the origin of this divergent term by looking at the usual soft photon expansion of the radi-

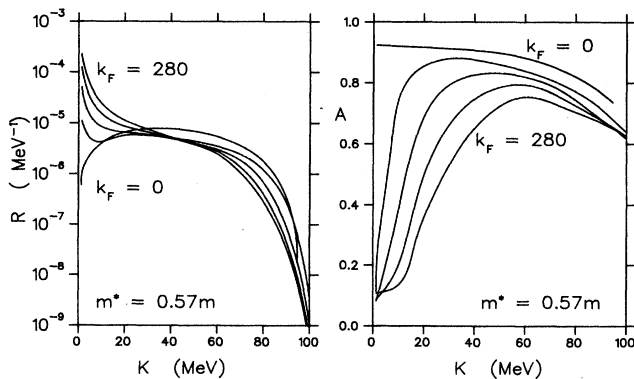


FIG. 5. Same as Fig. 4 except that the full photon range is shown.

ative amplitude.^{19,20} This gives for the radiative amplitude M_{fi}^{rad}

$$M_{fi}^{\text{rad}} = \left[\frac{\epsilon \cdot \mu}{k \cdot \mu} - \frac{\epsilon \cdot p}{k \cdot p} \right] M_{fi}^{\text{ord}} + O(1) + O(k) + \dots, \quad (7)$$

where ϵ is the photon polarization vector. In the transverse gauge with the muon at rest

$$M_{fi}^{\text{rad}} \rightarrow \frac{\epsilon \cdot p}{k \cdot p} M_{fi}^{\text{ord}} + \dots \rightarrow \frac{\epsilon \cdot p}{km} M_{fi}^{\text{ord}} + \dots, \quad (8)$$

where the last expression is obtained by expanding, as is usually done in nonrelativistic calculations, in powers of p/m .

One can see from this expression that for a proton at rest this $1/k$ term in the amplitude vanishes exactly, and thus one gets the usual spectrum which vanishes at $k = 0$. Once Fermi motion is included, however, such terms should be there. In the usual nonrelativistic calculations only the single term above survives since all higher terms in $1/m$ are dropped. This term was actually noted by Rood and Tolhoek¹¹ but discarded as small in the interesting region.

One of the virtues of the full relativistic calculation is that such terms can be included to all orders, and we can see how large they are. Figure 6 shows the contributions of the square of the $1/k$ term given in Eq. (7) above and also the full result obtained when this contribution to the amplitude is simply dropped, which amounts to removing both the square of the $1/k$ term and its interference with the nondivergent pieces. Figure 7 shows the same thing in the experimentally accessible region. These terms are clearly responsible both for the entire rate and for the behavior of the asymmetry parameter in the small k region. In the region above 60 MeV the contribution of these terms to the rate is very small, apparently because of a

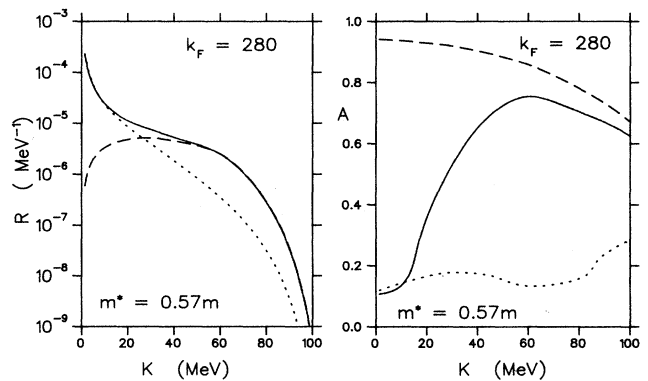


FIG. 6. Relative rate and asymmetry parameter for $k_F = 280$ MeV and $m^* = 0.57m$. The solid curve is the full result. The dotted curve shows the contribution of the square of the $1/k$ part of the amplitude. The dashed curve is the full result minus both the square of the $1/k$ part of the amplitude and the interference of this $1/k$ term with the remaining nondivergent part of the amplitude. It thus corresponds to the result obtained by dropping all divergent parts of the amplitude, as is usually done in nonrelativistic calculations.

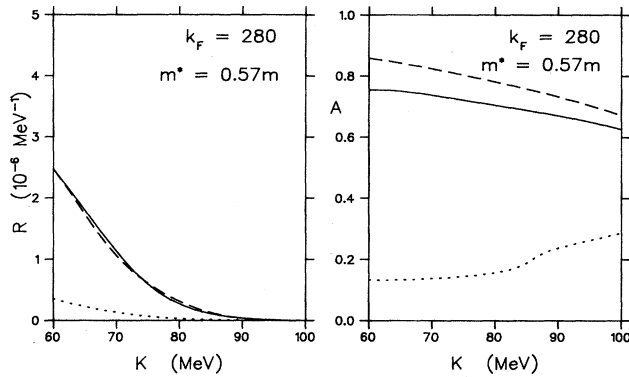


FIG. 7. Same as Fig. 6 except only the experimentally accessible region is shown.

destructive interference between the $1/k^2$ and the $1/k$ terms. The asymmetry parameter would be increased by about 10%, however, if these $1/k$ terms are dropped.

To understand whether the effects discussed here are interesting one has to understand how radiative muon capture is used. In most cases experiment is compared to theory with the aim of extracting the weak coupling constants, particularly the induced pseudoscalar coupling g_p . If a different theory is used or if some terms are neglected, one simply extracts a different value of g_p from the data. To first order most corrections and additions to the theoretical predictions seem to change mainly the magnitudes, as does changing g_p . Thus, while in the future more accurate experiments may obtain information from details of the changes in shape, one can get an idea of the importance of various corrections simply by comparing the change they make in the magnitude of the rate or asymmetry parameter with the changes made by changing g_p by some amount.

To make this comparison possible we thus show in Fig. 8 the relative rate and asymmetry for a range of values of g_p . By comparing this figure with the preceding ones we can get an idea of the effect on the extraction of g_p of the various corrections we have considered. The largest, what we have called the Fermi motion effect, really includes a number of relativistic effects. Clearly the result would be completely wrong if all such effects were neglected. However, essentially all nonrelativistic calculations which use realistic nuclear wave functions will have included some Fermi motion effects, via p/m pieces of the operator. Terms of order $(p/m)^2$ used in the usual nonrelativistic calculations were found earlier to be important at the level of only about $1 \times g_A$ in the extraction of g_p .⁹ The present calculation includes such effects to all orders and likewise similar effects from the wave functions. While we cannot separate those pieces which are normally included already in nonrelativistic calculations from those that are not, the fact that the sum of such terms is very important suggests that a careful treatment of a relativistic model may also be important.

The specific changes introduced by the replacement $m \rightarrow m^*$ could affect the value of g_p extracted from the rate by something of the order of 80% at 70 MeV and

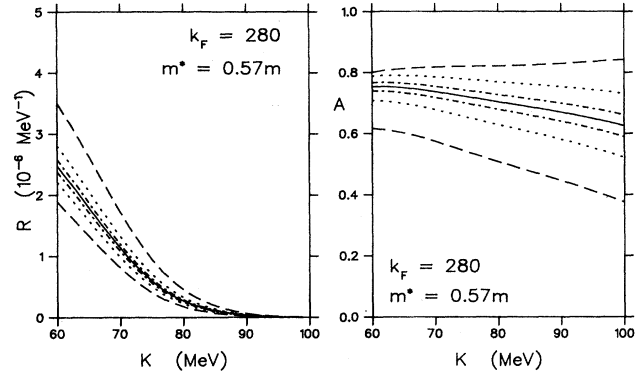


FIG. 8. Relative rate and asymmetry parameter for $k_F = 280$ MeV and $m^* = 0.57m$ as a function of the induced pseudoscalar coupling g_p . Shown are results for cases with the Goldberger-Treiman value of g_p multiplied by factors 0.2, 0.7, 0.9, 1.0, 1.1, 1.3, and 1.8. Thus the dot-dashed, dotted, and dashed curves correspond respectively to changes in g_p of $\pm 10\%$, $\pm 30\%$, and $\pm 80\%$. Over this range of values the rate increases uniformly with increasing g_p , while A decreases.

from the asymmetry by 20–30%, as can be seen by comparing Figs. 3 and 8. The inclusion of the $1/k$ terms affects the rate negligibly but would affect g_p obtained from the asymmetry by amounts ranging from the order of 80% at 70 MeV to 20% at 100 MeV. Thus in both cases it is clearly important to include these effects if one is to extract a reliable value of g_p .

The combined effect of the relativistic and m^* terms considered here is a suppression of the rate in the experimental region. A similar reduction can also be obtained by reducing the numerical value of g_p . Thus the value of g_p extracted from data analyzed using theories not containing these terms would be somewhat lower than that which would be obtained if such terms are included. It is interesting, and perhaps suggestive, that current data analyzed using standard nonrelativistic theories¹⁵ does seem to indicate such a quenching of g_p in heavy nuclei.

VI. CONCLUSIONS AND SUMMARY

We have examined radiative muon capture in the nuclear medium in the context of a relativistic Fermi gas model and using relativistic mean field theory to generate the single-particle wave functions. Such a model does not give a quantitative description of finite nuclei. Our aim, however, was not such a description, but instead an exploration of various effects of such relativistic models, particularly the consequences of an effective mass $m^* \leq m$. The intention was to determine whether there were significant effects which would warrant a more detailed calculation in a relativistic model appropriate for finite nuclei.

We found that the most important effects were those due to the initial proton not being at rest. Effects arising from the effective mass in the nuclear medium and some interesting consequences of the divergent term in the amplitude were also explored. A number of these effects could modify the value of g_p extracted from a given ex-

periment by significant amounts, of the order of several times g_A . Thus they are well within the interesting region, even for present experiments, but most certainly for future higher precision ones. This suggests that it is indeed appropriate to examine such relativistic effects in more detail and in a model relevant for finite nuclei. It would also be interesting to explore in such a calculation the consequences of using an effective pseudovector πNN interaction, a question which has not been addressed at all in the present investigation. Such an interaction leads to the same axial weak current for nucleons as does the

pseudoscalar interaction, even in the presence of uniform mean fields.³ It could, however, generate additional terms in the matrix element when combined with the electromagnetic interaction, as required for radiative muon capture. Furthermore, for finite nuclei there may be other interesting differences worth investigating, as found for other situations.³

This work was supported in part by grants from the Natural Sciences and Engineering Research Council of Canada and from the U.S. National Science Foundation.

-
- ¹B. D. Serot and J. D. Walecka, in *Advances in Nuclear Physics*, edited by J. W. Negele and E. Vogt, (Plenum, New York, 1986), Vol. 16, p. 1, and references cited therein.
- ²See, for example, L. G. Arnold *et al.*, Phys. Rev. C **19**, 917 (1979); L. G. Arnold *et al.*, *ibid.* **23**, 1949 (1981); J. R. Shepard *et al.*, Phys. Rev. Lett. **50**, 1443 (1983).
- ³M. W. Price and G. E. Walker, Phys. Rev. C **38**, 2860 (1988); M. W. Price, Ph.D. thesis, University of Indiana, 1986 (unpublished).
- ⁴J. A. McNeil *et al.*, Phys. Rev. C **34**, 746 (1986).
- ⁵T. Suzuki, Phys. Lett. B **175**, 257 (1986).
- ⁶R. J. Furnstahl and B. D. Serot, Nucl. Phys. **A468**, 539 (1987).
- ⁷H. W. Fearing, Phys. Rev. C **21**, 1951 (1980).
- ⁸D. S. Beder and H. W. Fearing, Phys. Rev. D **35**, 2130 (1987).
- ⁹R. S. Sloboda and H. W. Fearing, Nucl. Phys. **A340**, 342 (1980).
- ¹⁰R. S. Sloboda and H. W. Fearing, Phys. Rev. C **18**, 2265 (1978).
- ¹¹J. R. Luyten, H. P. C. Rood, and H. A. Tolhoek, Nucl. Phys. **41**, 236 (1963); H. P. C. Rood and H. A. Tolhoek, Nucl. Phys. **70**, 658 (1965).
- ¹²H. W. Fearing, Phys. Rev. **146**, 723 (1966).
- ¹³L. L. Foldy and J. D. Walecka, Nuovo Cimento **34**, 1026 (1964).
- ¹⁴M. Gmitro and P. Truöl, in *Advances in Nuclear Physics*, edited by J. W. Negele and E. Vogt (Plenum, New York, 1987), Vol. 18, p. 241.
- ¹⁵A. Frischknecht *et al.*, Phys. Rev. C **32**, 1506 (1985); **38**, 1996 (1988); M. Döbeli *et al.*, *ibid.* **37**, 1633 (1988); C. J. Virtue, Ph.D. thesis, University of British Columbia, 1987 (unpublished); M. D. Hasinoff *et al.*, in Vol. II, Contributed Abstracts, Proceedings of the 10th International Conference on Particles and Nuclei, Heidelberg, 1984, edited by F. Güttner, B. Povh, and G. zu Pulitz.
- ¹⁶G. Azuelos and M. Hasinoff, spokesmen, TRIUMF Experiment No. 452.
- ¹⁷J. C. Sens, Phys. Rev. **113**, 679 (1958).
- ¹⁸H. W. Fearing, Phys. Rev. Lett. **35**, 79 (1975).
- ¹⁹F. E. Low, Phys. Rev. **110**, 974 (1958).
- ²⁰T. H. Burnett and N. M. Kroll, Phys. Rev. Lett. **20**, 86 (1968).